Crosslinking Mechanism of Boric Acid with Diols Revisited

Marcel Rietjens*[a,b] and Peter A. Steenbergen[a,c]

Keywords: Boric acid / Borate / Diols / Guaran / Crosslinking / Rheology

Complex formation of boric acid with diol functional groups is well known and many papers have been published assuming borate is the reactive species. Based on the high reactivity of boric acid towards nucleophiles, this paper assumes boric acid is the reactant. We prove this hypothesis by presenting a study of the reaction of the polymer guaran with boric acid under various conditions. A thermodynamic analysis of the underlying reactions does not show any differences between either crosslinking species. Thermodynamics shows that the concentration of the 2:1 crosslinks, that give rise to the enhanced viscosity, is proportional to [B], the boric acid concentration, [X^2], the concentration of available crosslink sites and inversely proportional to [H^+]. These predictions were all confirmed by experiment. However, a difference between the mechanisms is demonstrated in a kinetic analysis: Longer gel times are predicted with the mechanism based on boric acid as the pH of the fluid increases, that is exactly what is observed in practice. Evidence is provided from visco-elastic measurements. A new approach to describe inter- and intramolecular crosslink formation is introduced and evidence for the correctness of this description is provided.

Introduction

Gelled fluids based on the natural polysaccharide guaran, crosslinked with for example borate, are generally used to fracture oil and gas wells to improve productivity. These fractures start at the well bore and can extend up to several hundred meters into the formation. Basically, this process tremendously increases the surface area of the well bore. In the preparation of borate crosslinked gels, pH (control) is crucial to the success of fracture treatments. The effects of pH and temperature on borate equilibriums have been well described and summarized by Harris.[1] Interestingly, when these gels are prepared the crosslink time depends on the pH of the solution: the higher the pH, the longer it takes to form a gel. At a pH value of 12 and above, the crosslink time may be an hour or longer. This cannot be explained by assuming borate as the reactive species. An additional interesting feature of borate crosslinked gels is their self-healing property: i.e. when exposed to high shear stresses, the network breaks up (shear thinning) but reheals quickly when it comes to rest.[1–3]

Guaran consists of a (1→4) linked mannosepyranosyl backbone with single galactosepyranosyl units connected by (1→6) linkages. The ratio between mannose and galactose is about 2:1.[4,5] Both monomers are capable of forming complexes with boric acid. The complex formation constant strongly depends on the stereochemistry of the diol functionality and their relative positions, 1,2 or 1,3. These aspects have been treated in detail by van den Berg et al.[6] Nuclear Magnetic Resonance (NMR) experiments have shown that complex formation constants of 1,2-diols are larger than 1,3-diols whereas 1,2 complex formation constants of mannose and galactose 1:1 complexes are comparable.[7,8] Combined with the known ratio of mannose to galactose in guaran, boric acid preferentially forms crosslinks with mannose in a ratio of 2:1 in agreement with experiment.[5]

Many authors have assumed borate is the reactive species[1,2,5,8–15] while others have assumed cations to be involved.[14] In a few cases boric acid was proposed as the reactant but merely because the reactions took place at very low pH values.[13] Tetraborate was assumed to be the crosslinking reactant by Khomutov et al., which is more in line with the proposed mechanism covered in this paper because it contains trivalent boron.[16] Van Duin[17,18] realized, based on similar arguments as given below, that boric acid could also be the reactive species and takes both boric acid and borate into account in the reaction equations.

In principle, reaction of an alcoholic group with borate is similar to the formation of an ether and requires dehydration. These types of reactions require time and specific conditions such as heat, to overcome the activation energy, and the removal of water. Properties like self-healing and the fact that equilibrium between boric acid and borate is faster than the NMR time scale can only be explained provided the reactions are fast, in contradiction with the above observations for ether formation. Thus the reaction must

[a] Halliburton,
Treubstraat 1H, 2288 EG Rijswijk, Netherlands
[b] Current address: Cimcool Industrial Products B.V.,
Schiedamsedijk 20, 3134 KK, Vlaardingen,
E-mail: marcel.rietjens@tiscali.nl
[c] Current address: Panterra Geoconsultants,
Leiderdorp, The Netherlands
E-mail: p.steenbergen@panterra.nl

have a very low activation energy. A determination of this latter value shows that it is indeed low and was reported to be 20.5 kJ/mol.[15] The trivalent B atom in boric acid has an empty p orbital that is very electrophilic in nature; it rapidly reacts with various nucleophiles to form complexes.[19] Therefore, a much more likely alternative mechanism is to assume boric acid as the reactant.

Theory

First, the two models based on boric acid and based on borate will be described. We assume that all crosslink sites are available for reaction and, for the moment, we do not differentiate between inter- and intramolecular crosslinks (Mxl). This issue will be dealt with later because we are primarily interested in the concentration of inter-Mxls because these give rise to visco-elasticity. We further assume similar behavior of guar (G) and hydroxypropylguar (HPG). Thus values for K_1 and K_2 are expected to be similar in magnitude. In the equations below, the following abbreviations are used:

X: Free crosslink site on guar polymer chain

B: $B(OH)_3$

B^-: $B(OH)_4^-$

X_1B/X_1B^-: 1:1 Complex with B in the boric acid/borate form crosslinked with one guar chain.

X_2B^-: 2:1 Complex in which two guar chains are crosslinked by one borate molecule and which is always negatively charged. X_2B^- includes both inter- and intramolecular crosslinks.

Boric Acid as the Reactive Species. Thermodynamics: The fundamental equilibriums are:

$$B + H_2O \rightleftarrows B^- + H^+ \quad (1a)$$

$$B + X \underset{k_{-1}}{\overset{k_1}{\rightleftarrows}} X_1B^- + H^+ + H_2O \quad (2a)$$

$$X_1B^- + H^+ \rightleftarrows X_1B + H_2O \quad (3a)$$

$$X_1B + X \underset{k_{-2}}{\overset{k_2}{\rightleftarrows}} X_2B^- + H^+ + H_2O \quad (4a)$$

Further, the mass balance is given by:

$$[B_{total}] = [B_t] = [B] + [B^-] + [X_1B] + [X_1B^-] + [X_2B^-] \quad (5a)$$

When substituting the expressions for B^-, X_1B^- etc. into Equation (5a) and rearranging we get:

$$[B_t] = [B]\cdot\left[1 + \frac{K_a}{[H^+]} + \frac{K_1\cdot[X]}{[H^+]} + \frac{K_1\cdot[X]}{K_a^{1:1}} + \frac{K_1\cdot K_2\cdot[X^2]}{[H^+]\cdot K_a^{1:1}}\right] = [B]\cdot M \quad (6a)$$

here K_a is the acid dissociation constant of boric acid, $K_a^{1:1}$ the acid dissociation constant of the complex X_1B, K_1 the equilibrium constant for the formation of the 1:1 complex and K_2 the formation constant of the 2:1 complex. The concentration of 2:1 complexes is then given as:

$$[X_2B^-] = \frac{K_1\cdot K_2\cdot[B_t]\cdot[X^2]}{[H^+]\cdot K_a^{1:1}\cdot M} \quad (7a)$$

Equation (7a) is the fundamental thermodynamic expression that describes the concentration of the 2:1 crosslinked products as a function of X, B and pH.

Borate Anion as the Reactive Species. Thermodynamics: In this case Equation (2a) and (4a) are defined as:

$$B^- + X \underset{k_{-1}}{\overset{k_1}{\rightleftarrows}} X_1B^- + 2H_2O \quad (2b)$$

$$X_1B^- + X \underset{k_{-2}}{\overset{k_2}{\rightleftarrows}} X_2B^- + 2H_2O \quad (4b)$$

The mass balance is now defined as:

$$[B_t] = [B^-]\cdot\left[\frac{[H^+]}{K_a} + 1 + \frac{K_1\cdot[H^+]\cdot[X]}{K_a^{1:1}} + K_1\cdot[X] + K_1\cdot K_2\cdot[X^2]\right] = [B^-]\cdot N \quad (6b)$$

The concentration of 2:1 complexes is now given by:

$$[X_2B^-] = \frac{K_1\cdot K_2\cdot[B_t]\cdot[X^2]}{N} \quad (7b)$$

Equation (7a) and (7b) show $[X_2B^-]$ is linear in $[X^2]$ and $[B_t]/M$ or $[B_t]/N$ in both models. In fact Equation (7a) and (7b) are exactly equivalent and therefore thermodynamics *cannot* differentiate between both mechanisms.

Boric Acid as the Reactive Species. Kinetics: The basic general rate equations for the formation of 1:1 and 2:1 complexes are:

$$Rate = \frac{d([X_2B^-])}{dt} = k_2\cdot[X_1B]\cdot[X] - k_{-2}\cdot[X_2B^-]\cdot[H^+] \quad (8a)$$

$$\frac{d([X_1B])}{dt} = k_{-a}^{1:1}\cdot[X_1B^-]\cdot[H^+] - k_a^{1:1}\cdot[X_1B] - k_2\cdot[X]\cdot[X_1B] + k_{-2}\cdot[X_2B^-]\cdot[H^+] \quad (9a)$$

$$\frac{d([X_1B^-])}{dt} = k_1\cdot[B]\cdot[X] - k_{-1}\cdot[X_1B^-]\cdot[H^+] - k_{-a}^{1:1}\cdot[X_1B^-]\cdot[H^+] + k_a^{1:1}\cdot[X_1B] \quad (10a)$$

A steady state is assumed for the formation of X_1B and X_1B^-. In other words $d([X_1B])/dt = d([X_1B^-])/dt = 0$. The justification for these assumptions is that reaction rates in-

volving free boric acid, which is a small molecule, are much greater than reaction rates involving two polymer chains.

An expression for $[X_1B]$ in terms of [B], [X] and $[X_2B^-]$ can now be derived from Equation (9a) and (10a). Substitution in Equation (8a) yields:

$$\frac{d([X_2B^-])}{dt} = C_1 + C_2 \cdot [X_2B^-] \quad (11a)$$

with

$$C_1 = \frac{k_{-a}^{1:1} \cdot k_1 \cdot k_2 \cdot [B] \cdot [X^2]}{k_{-1} \cdot k_a^{1:1} + k_{-1} \cdot k_2 \cdot [X] + k_{-a}^{1:1} \cdot k_2 \cdot [X]} \quad (12a)$$

and

$$C_2 = \frac{(k_{-1} \cdot k_{-2} + k_{-a}^{1:1} \cdot k_{-2}) \cdot k_2 \cdot [X] \cdot [H^+]}{k_{-1} \cdot k_a^{1:1} + k_{-1} k_2 \cdot [X] + k_{-a}^{1:1} \cdot k_2 \cdot [X]} - k_{-2} \cdot [H^+] \quad (13a)$$

After applying the initial condition $X_2B^- = 0$ for $t = 0$, the solution of Equation (11a) is:

$$[X_2B^-] = \left(e^{C_2 \cdot t} - 1\right) \cdot (C_1 / C_2) \quad (14a)$$

Borate Anion as the Reactive Species. Kinetics: The derivation is very similar and the solution of the differential equations has the same form with C_1 and C_2 expressed as:

$$C_1 = \frac{k_1 \cdot k_2 \cdot [B^-] \cdot [X]^2}{k_{-1} + k_2 \cdot [X]} \quad (12b)$$

$$C_2 = \frac{k_2 \cdot k_{-2} \cdot [X]}{k_{-1} + k_2 \cdot [X]} - k_{-2} \quad (13b)$$

As t approaches infinity, both kinetic expressions yield the thermodynamic relation. The main difference is that the term C_2 is independent of pH in the borate model whereas it is a function of pH in the boric acid model.

Results and Discussion

In the calculations and discussions that follow we introduce [X*], the critical concentration of crosslink sites in mol/L, similarly defined as the critical overlap concentration of a polymer, [P*]. Likewise, the concentrations of 1:1 and 2:1 complexes are expressed in mol reacted crosslink sites/L. In plots or when dealing with critical concentrations, we sometimes use the polymer concentrations [P] and [P*] in g/L because these are more familiar in use. No precautions were made to minimize effects due to charge repulsion by the addition of salt.

Chemistry of Borate Complexes: Both 1,2- and 1,3-diols can form 1:1 and 2:1 complexes with boric acid. Each reaction is assumed to proceed in two steps, and because the second step, ring closure, is relatively fast due to the chelate effect, the first step is rate limiting.[17] Paál[20,21] discusses effects of induction, solvation, and H-bonding, in the case that multiple OH groups are present, on the value of K_1. Boric acid complexes with 1,2-diols are well known to possess higher acidities as opposed to 1,3-diols.[15,21,22] The stronger acidity is primarily caused by ring strain. Complexes formed from 1,3-diols form six rings and are slightly more acidic compared to boric acid[15,22] but complexes from 1,2-diols are five rings and have considerable ring strain. In the neutral form, the hybridization of the B nucleus is sp^2 vs. sp^3 in the borate form. In the transition to the borate form, the ring strain is relieved and the activation energy decreases to even lower values.

The stability of 1:1 and 2:1 borate complexes has been shown to be optimum in a certain pH range. Below and above this range no complexes are formed.[17,23] The reason that has been forwarded at high pH values, > 13, is charge repulsion because of deprotonation of the diol group.[13,23] Although we propose compounds containing trivalent boron, B and X_1B, as the reactant species, B and X_1B are still in rapid equilibrium with B^- and X_1B^- respectively. As a consequence, the boron nucleus will be negatively charged on average and therefore subject to charge repulsion.

Inter/intramolecular Crosslinking: In the derivation of the equations above no account was given to inter- and intra-Mxls. Because visco-elasticity is a function of the concentration of inter-Mxl only this must be incorporated in the model. We assume that the polymer coils have a fixed radius of gyration that is independent of the polymer concentration. Thus at [P] > [P*] the coils mix instead of compressing each other. The first step, formation of the 1:1 complex, is the same for both inter- and intra-Mxls. Basically, this formation is a reaction between a crosslink site and boric acid. Because the latter is able to move freely throughout the fluid, all potential crosslink sites are available for reaction. The concentration of 1:1 complexes is than proportional to [X]·[B].

The formation of 2:1 intra-Mxl complexes is a reaction between a 1:1 complex and a free crosslink site in the same polymer chain. At [P] < [P*], the available number of crosslink sites equals the number of crosslink sites within the individual coil. Effectively, this is the same (bulk) concentration as when the coils just touch each other, i.e. at [P] = [P*]. Therefore, the effective concentration of crosslink sites within each coil is equal to [X*]. For intra-Mxls, this relation applies also to concentrations above [P*] because we have assumed the radius of gyration as constant and because reaction with other coils are counted separately as inter-Mxls. Therefore, the concentration of intra-Mxls is proportional to [X]·[X*].

At [P] > [P*] coils of different polymer chains touch each other and reactions between different polymer coils lead to inter-Mxls. Formation of inter-Mxls are assumed to commence at [P] > [P*]. As with intra-Mxls, inter-Mxls are the reaction products from a 1:1 complex and an available crosslink site. Now the number of available crosslink sites is proportional to ([X] – [X*]) because only that portion is able to react with other coils. It follows that the concentration of inter-Mxls is proportional to [X]·{[X] – [X*]}. The ratio of inter- and intra-Mxls is then simply calculated as {[X] – [X*]}/[X*] and is > 0 at [P] > [P*]. However, at polymer concentrations higher than P* deviations can be

anticipated. For example, due to excluded volume effects, compression of the coils can be expected to some extent. This leads to an effective higher concentration of P*. Overall, the concentration of 2:1 complexes can be calculated as the sum of inter- and intra-Mxls and is proportional to $[X]^2$ [see Equation (7a)]. The fractions F of the inter- and intra-Mxls are calculated as:

$$F_{Inter} = \frac{P - P^*}{P} \quad (15a)$$

$$F_{Intra} = \frac{P^*}{P} \quad (15b)$$

having a ratio of

$$\frac{Inter}{Intra} = \frac{P - P^*}{P^*} \quad (15c)$$

Pezron et al. derived a different equation for the ratio between inter- and intra-Mxls.[9] They relate a critical concentration C_0 to the average size of a loop or an intra-Mxl. The ratio inter/intra is calculated as $(C/C_0)^{5/4}$. For guar of similar molecular weight they assessed a value for C_0 of 4%. In their view, the concentration of inter-Mxls is always > 0, assuming a $[P] > 0$, and steadily grows. However, even at a polymer concentration twice as large as [P*], the ratio is barely 0.05, whereas in our case it is 1, that is twenty times as large. This issue is further discussed in the model parameter section that follows. We do agree with the statement of Pezron et al. that the ratio inter/intra is dependent on the flexibility of the polymer coils. The more flexible, the closer the segments are to each other favoring intra-Mxl. In our view this is accounted for in the higher value of [P*] because a more flexible coil has a smaller radius of gyration.

Model Parameters: We have deduced the model parameters from first principles and available date of equilibrium constants published in the literature. Further, we have applied the concept of reduced diffusion coefficient in analogy with the reduced mass and is defined as: $D_{reduced} = D_1 + D_2$, where D_1 and D_2 are the diffusion coefficients of the species 1 and 2.

***K*$_a$:** The equilibrium between boric acid and borate is known to be very fast, even faster then the NMR time scale. The reverse rate constant, k_{-a}, was determined by Gilkerson as $1.3 \cdot 10^{10}$ L·mol^{-1}·s^{-1}.[24] Based on this value and the known value of K_a of boric acid,[25] $5.8 \cdot 10^{-10}$ mol·L^{-1}, the forward rate constant, k_a, is calculated as 7.5 s^{-1}. The value of k_{-a} will be used as a basis for the rate constants k_{-1} and k_{-2}.

[P], [P*]: The critical concentration P* was determined by measuring G' as a function of [P] down to the lowest measurable concentration of 1.7 g/L, with and without additional crosslinker. The value of [P*] was taken as the concentration where the two curves merge and was assessed at 2.04 g L^{-1}. This value is in good agreement with published values.[5]

[X], [X*]: At a polymer concentration of 3 g/L, the concentration of [X] is calculated as $0.73 \cdot 3/179 = 0.012$ mol·L^{-1}. The average Mw of a monomer in HPG is about 179 and 0.73 is the fraction of crosslink sites available per monomer due to the HP groups. The value of X* is 0.0083 mol·L^{-1}.

***K*$_1$, *k*$_{-1}$, *k*$_1$:** The value for k_{-1} is deduced from k_{-a}. Three effects influence its value: 1) Compared to the borate anion, which has four OH groups, the 1:1 complex has two OR groups thus a statistical chance of 2/4 to become protonated followed by elimination of H_2O. 2) Compared to OH groups, OR groups have a twofold lower basicity thus have equally less chance to become protonated.[26] 3) The 1:1 complex dissociates into boric acid and a polymer chain and, compared to water, as in the reverse reaction of B^- to B, boric acid has a roughly threefold smaller diffusion coefficient. In summary, the value of k_{-1} is calculated as $1.3 \cdot 10^{10}/(2 \cdot 2 \cdot 3) = 1.08 \cdot 10^9$ L·mol^{-1}·s^{-1}. The value of the equilibrium constant K_1 is calculated from literature data based on dialysis measurements: $K'_1 = 11$ L·mol^{-1} and is defined as $K'_1 = [X_1B^-]/([B^-] \cdot [X])$.[8] In this paper K_1 is defined as $K_1 = [X_1B^-] \cdot [H^+]/([B] \cdot [X])$. Because $K_1 = K'_1 \cdot K_a$ its value is $6.4 \cdot 10^{-9}$. The value of k_1 is then calculated as 6.9 L·mol^{-1}·s^{-1}.

***K*$_a^{1:1}$, *k*$_{-a}^{1:1}$, *k*$_a^{1:1}$:** The acidity of the (neutral) 1:1 complex is defined by $K_a^{1:1}$. Its value is required to calculate K_2. It is well known that the acidity of boric acid increases upon the addition of a 1,2-diol. Sugars such as mannitol and sorbitol are widely used for this purpose in analytical chemistry. Based on titration data with these sugars, apparent K_a values were calculated for boric acid complexes.[27] Based on these data, we estimate an apparent $K_a^{1:1}$ value for the 1:1 complex of $1 \cdot 10^{-5}$ mol·L^{-1}. The absolute value is in fact not relevant for the calculated crosslink density because $K_a^{1:1}$ cancels out in the equation for $[X_2B^-]$. However, it does point out that X_1B complexes are much more acidic and that the concentration of the neutral 1:1 complex decreases very rapidly with increasing pH. The value of $k_{-a}^{1:1}$ is based on the value of k_{-a}. Because there are two OH groups vs. four in borate, the statistical factor is 2/4. We neglect any effect on the basicity of the OH groups due to the complexed diol. Because the values of $k_a^{1:1}$ and $k_{-a}^{1:1}$ are of no concern for the result, ring strain caused by complexation with an 1,2-diol is accounted for only in an increase in the value of $k_a^{1:1}$, not in $k_{-a}^{1:1}$. The reduced diffusion coefficient is that for water and does not change. The value for $k_{-a}^{1:1}$ is then $1.3 \cdot 10^{10}/2 = 6.5 \cdot 10^9$ L·mol^{-1}·s^{-1} and $k_a^{1:1} = K_a^{1:1} \cdot k_{-a}^{1:1} = 6.5 \cdot 10^4$ s^{-1}.

***K*$_2$:** Similar to K_1 we can express K_2 as $K'_2 \cdot K_a^{1:1}$. Pezron[8] defined K'_2 as $K'_2 = [X_2B^-]/([X_1B^-] \cdot [X])$. Two sets of data are available that should allow for the calculation of K_2, NMR spectroscopic data and rheological data. Because the NMR spectroscopic data have a high level of uncertainty, we used the data based on rheological experiments.[2] A critical note to place is that these data have not been corrected for physical crosslinks (see below). The value of K'_2 was obtained from the slope of G' vs. $[P]^{2.6} \cdot [B^-]$ (Figure 6 in ref.[2]), although it is unclear why they have used a power

of 2.6 instead of 2. The same analysis, but based on a power of 2, yields a slightly better fit. Further, they state that the slope is equal to $2{\cdot}K'_2{\cdot}RT$ but substitution of the appropriate definitions for $[X_2B^-]$ in Equation (16) below, results in $2{\cdot}K'_1{\cdot}K'_2{\cdot}RT$. Using a power of 2.6 the value of K'_2 yields 0.43 mol·L^{-1} whereas with a power of 2 the value of K'_2 is only 0.09 mol·L^{-1}. Model calculations with a value of K'_2 = 0.09 mol·L^{-1} give smaller values for G' than observed experimentally and consequently the deviations, see Table 1, are < 1. The strange observation we then make is that the deviations become even larger (thus $<< 1$) in tests with higher polymer concentrations, whereas at higher polymer concentrations a gel behaves more rubber-like in line with model requirements. Therefore we have decided to use the value of 0.43 mol·L^{-1} instead. The value of K_2 is calculated as $4.3{\cdot}10^{-6}$.

In calculating the value of k_{-2}, the statistical factor is now 4/4 = 1, because there are four possibilities to break a bond of a diol as in B^-. The basicity is still twofold smaller than OH in B^-. At this point dissociation is between two polymer chains that have considerably smaller diffusion coefficients. From data of Brandrup,[28] the value of D for a guar sample with a M_w of 657.000 is $0.54{\cdot}10^{-11}$ m^2·s^{-1}. The molecular weight of the sample we used is approximately $2.0{\cdot}10^6$. Based on the data given in Brandrup, an empirical relation between D and M_w could be set up and based on this relation a value of D for the HPG sample used is calculated as 0.10 10^{-11} m^2·s^{-1}. Compared to the value for water ($D = 2.26{\cdot}10^{-9}$ m^2·s^{-1}), this value is about 2000-fold smaller. The value of k_{-2} is then calculated as $1.3{\cdot}10^{10}/(2{\cdot}2000) = 3.2{\cdot}10^6$ L·mol^{-1}·s^{-1}. From K_2 and k_{-2}, k_2 is finally calculated as 14 L·mol^{-1}·s^{-1}.

Physical Crosslinking: Solutions of guaran are very viscous and possess some degree of visco-elasticity caused by physical crosslinks or entanglements.[29] Because the model outlined above is based on chemical crosslinks, G' data must be corrected for contributions due to physical crosslinks (G'_{phys}). Experiments showed that physical crosslinks form very fast as plateau values were attained within few minutes. The value of G'_{phys} can be expected to be a function of polymer concentration and pH.[29] Figure 1 shows that the value of G'_{phys} is constant up to a pH of about 12, after which it decreases with increasing pH.

This observation is in line with data presented by Goycoolea et al.,[29] and is thought to be caused by charge up on the polymer chain due to deprotonation. In principle, the polymer behaves like a polyelectrolyte at very high pH values.[30] Assuming a pK_a value of 14.7 for the OH groups, it can be calculated that about 1% is dissociated at a pH value of 12.5.[26,30] The acquired charge leads to repulsion between chains, and therefore, partial disruption of the weak physical crosslinks. Charge up of the polymer is also caused by 1:1 complexes (the concentration of 2:1 complexes is relatively small). In the determination of the values for G'_{phys}, fructose was added to mask boric acid. A consequence is that 1:1 complexes are also not formed, whereas they are formed in the other experiments. This means that the values for G'_{phys} are overestimated, and therefore G′ values for chemical crosslinks are overcorrected. Model calculations, however, show that at the highest polymer and borate concentrations used, the concentration of 1:1 complexes is only 0.4% (relative to the total number of crosslink sites) so the magnitude of the overcorrection should be small. This observation is in agreement with calculations by Ochiai.[31] The effect of polymer concentration on G'_{phys} is shown in Figure 2.

In principle, one could expect G'_{phys} to be proportional to [P]·{[P] – [P*]}, the reason being similar to chemical

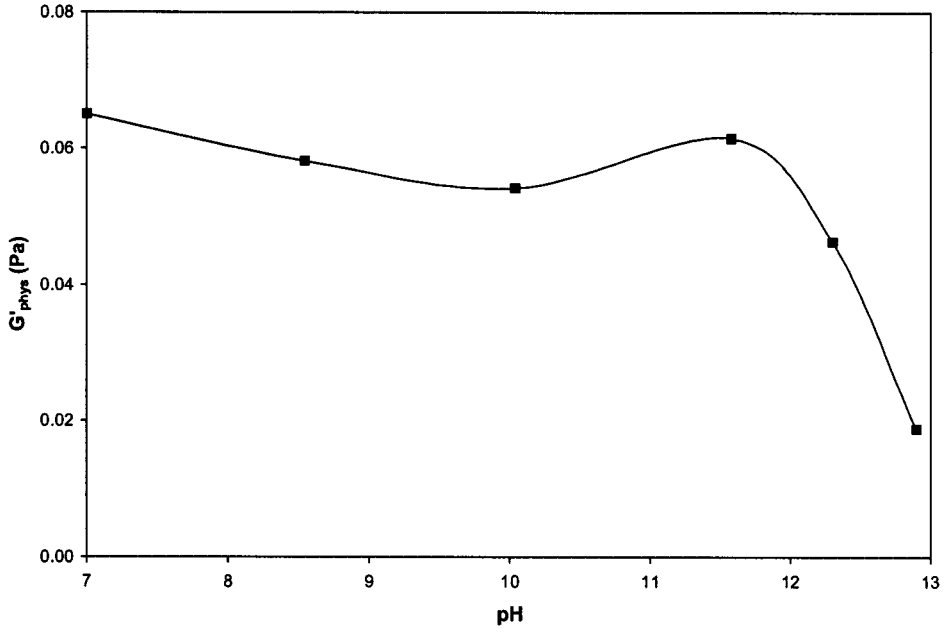

Figure 1. Effect of pH on visco-elasticity due to physical crosslinking.

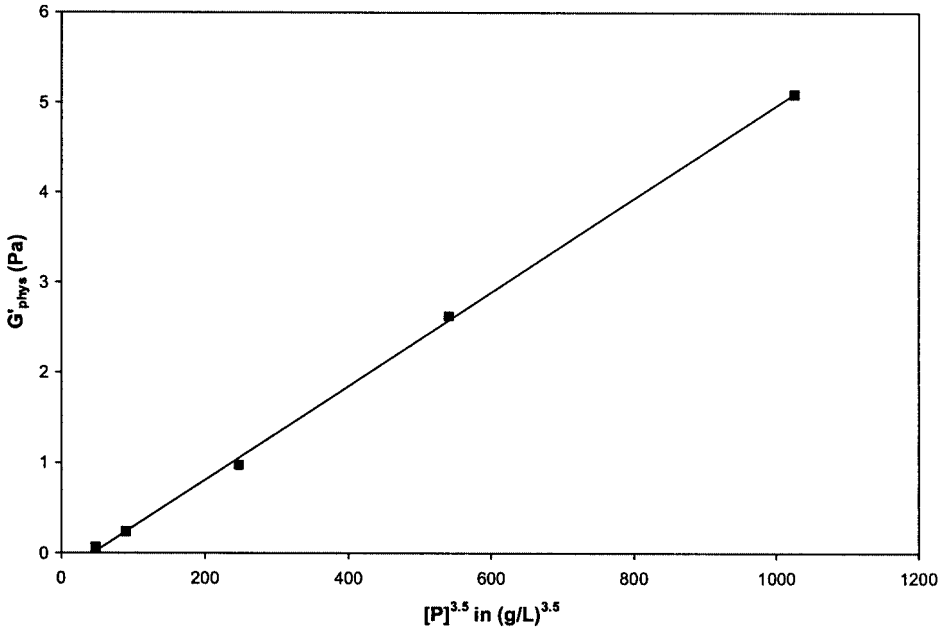

Figure 2. Effect of polymer concentration on visco-elasticity due to physical crosslinking.

crosslinking. This was not confirmed by an analysis, instead we found excellent correlations with the relations $G'_{phys} \approx [P]^{3.5}$ and $G'_{phys} \approx [P]^2 \cdot \{[P] - [P^*]\}$.

Model Validation. Thermodynamics: The dependence of G' as a function of total boron concentration is shown in Figure 3. Because these experiments were run at the same pH value, no account needed to be given to M. A straight line is observed in agreement with theory and published data.[2,3,14]

Equation (7a) further predicts a linear relationship between G' and $[P] \cdot \{[P] - [P^*]\}$. This relation is shown in Figure 4. This curve is clearly not linear but has some curvature because we assume

$$G' = 2\,[X_2B^-]_{Inter}RT \quad (16)$$

to be valid at very low values of G'. Schultz and Myers,[3] however, indicate that a minimum value for $[X_2B^-]_{inter}$ is required for this relation to be valid. Thus Equation (16) is true only if the gel behaves like an ideal rubber. The gels in our experiments have a very low crosslink density and cannot be considered a real rubber. However, this argument

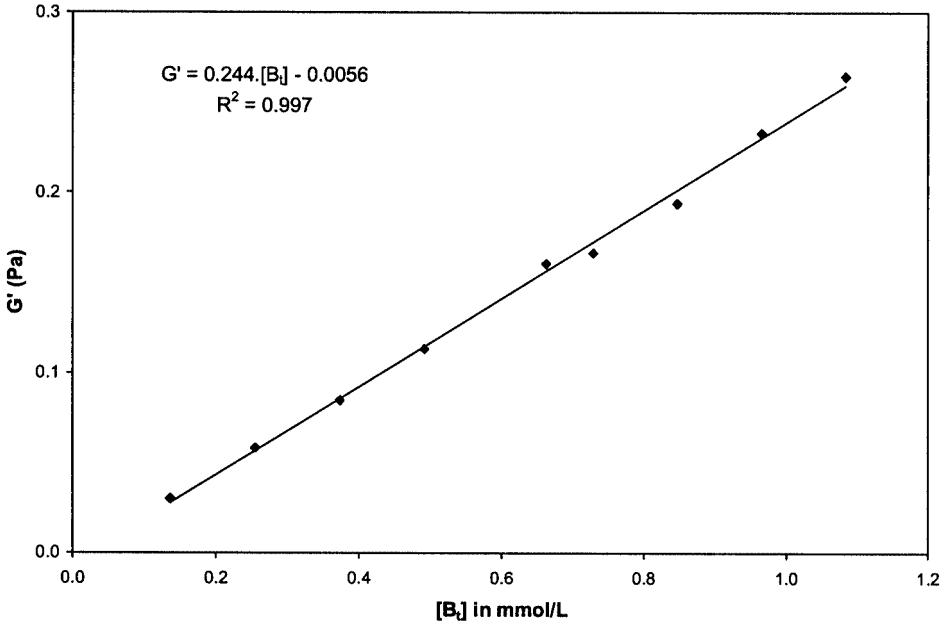

Figure 3. Correlation between visco-elasticity and total boron concentration; 3 g HPG/L, pH 10.04 ± 0.04.

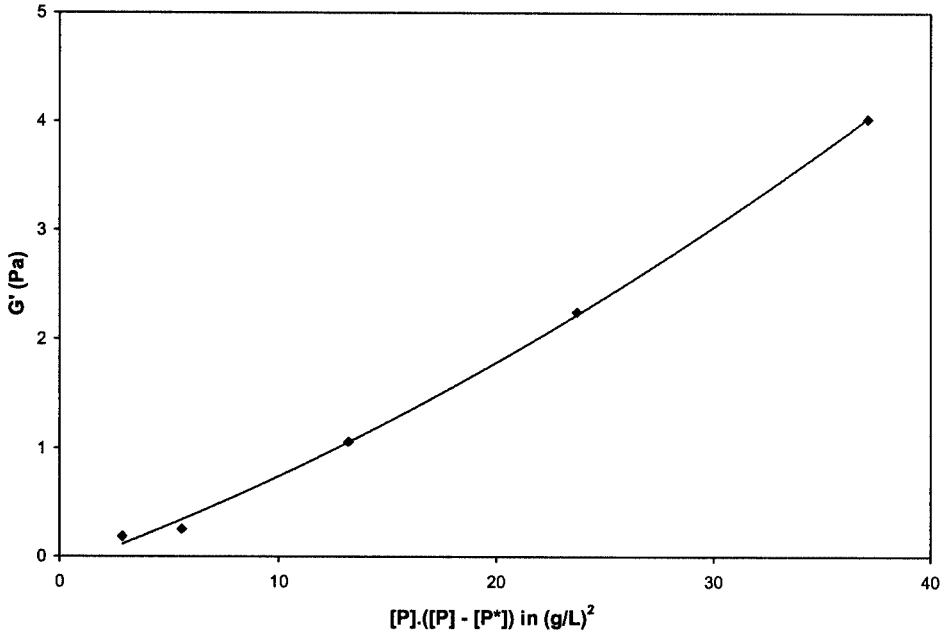

Figure 4. Correlation between visco-elasticity and [P]·([P] − [P*]); 300 μL crosslinker solution, pH 10.0 ± 0.08.

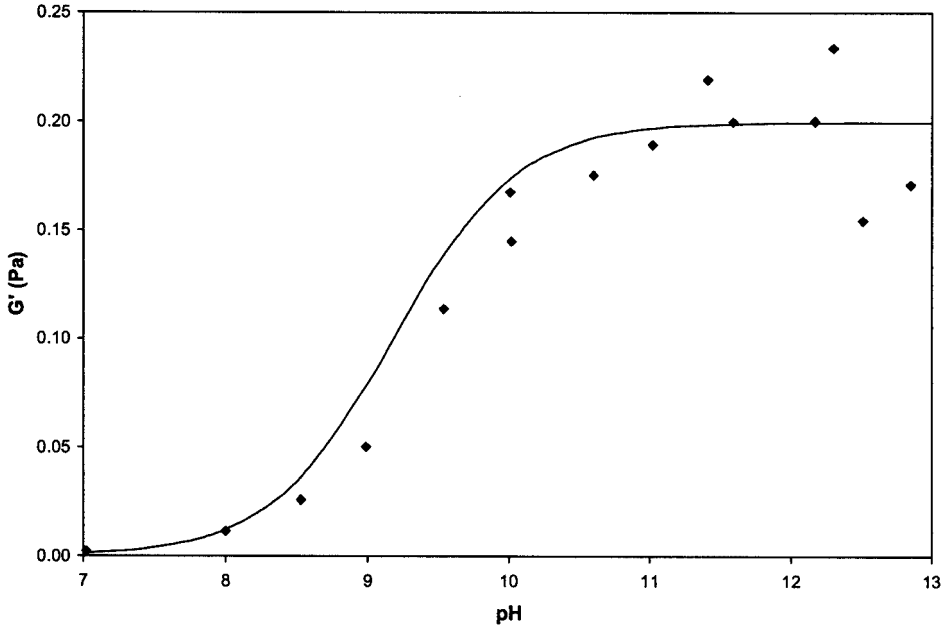

Figure 5. Visco-elasticity as a function of pH. The solid line is the theoretical curve with a deviation factor of 3.6 applied (see text); 500 μL crosslinker solution, [P] is 3 g/L.

is equally true for the data shown Figure 3. Because the corrections due to physical crosslinks in Figure 4 were up to 50% and were not a constant value, as opposed to data in Figure 3, and are subject to error also, the observed curvature may be misleading. Note that similar deviations from ideal behavior are shown in data published by Pezron et al. in gels with low B_t content and low polymer concentration: compare parts a–d in Figure 5 in ref.[2]

In Figure 5, G' is plotted as a function of pH at fixed concentrations of polymer and $[B_t]$. In the same Figure, the calculated model curve is included as well using a deviation factor of 3.6 (see later). Although there is some scatter in the experimental data at high pH values, the match with the theoretical curve is quite reasonable. Effects of deprotonation of the polymer chain could be anticipated at the highest pH value tested, 12.8, but because of the amount of scatter, it is difficult to state that the experimental curve drops below the theoretical curve. Experiments by van Duin et al.[23] do show that at deprotonation conditions, 0.5 M NaOH, the complex formation constant K_2 drops to zero

Table 1. Master Table showing the calculated and experimentally observed visco-elasticity values at the conditions specified. The deviation factor is defined as the theoretical value divided by the experimental value.

pH	$[B_t]$ (mol/L)	[P] (g/L)	[X] (mol xl sites/L)	# xl/ chain	$G'_{calcd.}$ (Pa)	$G'_{obsd.}$ (Pa)	Deviation
10.02	0.49	2.99	$1.22\cdot10^{-2}$	0.06	0.42	0.13	3.2
9.99	0.51	3.59	$1.47\cdot10^{-2}$	0.09	0.83	0.23	3.6
10.19	0.54	4.79	$1.96\cdot10^{-2}$	0.18	2.10	1.28	1.6
10.10	0.57	6.00	$2.45\cdot10^{-2}$	0.25	3.77	2.59	1.5
10.10	0.61	7.20	$2.94\cdot10^{-2}$	0.34	6.01	4.99	1.2
10.00	0.14	2.99	$1.22\cdot10^{-2}$	0.02	0.12	0.03	3.9
10.00	0.25	2.99	$1.22\cdot10^{-2}$	0.03	0.22	0.06	3.7
10.00	0.37	2.99	$1.22\cdot10^{-2}$	0.04	0.32	0.08	3.8
10.09	0.49	2.99	$1.22\cdot10^{-2}$	0.06	0.43	0.11	3.8
10.01	0.66	2.99	$1.22\cdot10^{-2}$	0.08	0.57	0.16	3.5
10.01	0.73	2.99	$1.22\cdot10^{-2}$	0.08	0.62	0.17	3.7
10.08	0.85	2.99	$1.22\cdot10^{-2}$	0.10	0.74	0.19	3.8
10.07	0.97	2.99	$1.22\cdot10^{-2}$	0.11	0.84	0.23	3.6
10.08	1.08	2.99	$1.22\cdot10^{-2}$	0.13	0.94	0.26	3.6
7.02	0.73	2.99	$1.22\cdot10^{-2}$	0.00	0.00	0.00	2.2
8.00	0.73	2.99	$1.22\cdot10^{-2}$	0.01	0.04	0.01	3.8
8.53	0.73	2.99	$1.22\cdot10^{-2}$	0.02	0.13	0.03	5.0
8.99	0.73	2.99	$1.22\cdot10^{-2}$	0.04	0.28	0.05	5.6
9.54	0.73	2.99	$1.22\cdot10^{-2}$	0.07	0.49	0.11	4.4
10.01	0.73	2.99	$1.22\cdot10^{-2}$	0.08	0.62	0.17	3.7
10.60	0.73	2.99	$1.22\cdot10^{-2}$	0.09	0.68	0.17	3.9
11.02	0.73	2.98	$1.22\cdot10^{-2}$	0.09	0.70	0.19	3.7
11.41	0.73	2.98	$1.22\cdot10^{-2}$	0.09	0.70	0.22	3.2
12.03	0.73	2.98	$1.22\cdot10^{-2}$	0.09	0.70	0.19	3.6
12.17	0.73	2.98	$1.21\cdot10^{-2}$	0.09	0.70	0.20	3.6
12.30	0.73	2.98	$1.21\cdot10^{-2}$	0.09	0.70	0.23	3.1
12.40	0.73	2.98	$1.21\cdot10^{-2}$	0.09	0.70	0.23	3.0
12.85	0.73	2.96	$1.21\cdot10^{-2}$	0.09	0.68	0.16	4.2

and estimates that effects of pH are noticeable at a pH > 13.

The data are summarized in Table 1. The deviation factor, defined as the ratio of calculated and observed values, is 3.6 on average but decreases to 1.2 in the experiments with the highest polymer concentration.

In Table 2 some data points published by Pezron et al.[2] are shown that were calculated through also. We used a molecular mass of $2.2\cdot10^6$ Daltons, a [P*] of 1.5 $g\cdot L^{-1}$, and assumed one crosslink site per monomer, each with a M_w of 156.[2] Even though the gels examined in their case were reasonably representative of a true rubber, the deviations from model calculations are quite similar to our results.

Model Validation. Kinetics: Figure 6 shows the results of model calculations of the concentration of X_2B^- vs. time. The calculated gel times vary from 100 seconds at a pH of 7 up to $10\cdot10^6$ seconds at a pH of 13. Compared to experimental data these numbers are about two orders in magnitude too large and are likely to be due to the estimated value for the diffusion coefficient D of polymer segments. The constant C_1 in Equation (14a) contains two terms but is in fact dominated by the last term: $k_{-2}\cdot H^+$. The value of k_{-2} is proportional to $D_{reduced}$ and the value used for guaran was calculated from sedimentation experiments. In such experiments, the entire molecule settles in a gravitational field, whereas the mobility of chain segments is expected to be

Table 2. Data from Pezron et al. re-calculated[2], see text for details.

pH	$[B_t]$ (mol/L)	[P] (g/L)	[X] (mol xl sites/ L)	# xl/ chain	$G'_{calcd.}$ (Pa)	$G'_{obsd.}$ (Pa)	Deviation
9.2	3.5	4.4	$2.8\cdot10^{-2}$	2	18	4	4.5
9.2	8.2	4.4	$2.8\cdot10^{-2}$	4	42	19	2.3
9.2	3.9	5.5	$3.5\cdot10^{-2}$	3	34	13	2.7
9.2	8.8	5.5	$3.5\cdot10^{-2}$	6	75	38	2.0
9.2	4.2	7.7	$4.9\cdot10^{-2}$	4	72	29	2.5
9.2	9.7	7.7	$4.9\cdot10^{-2}$	10	168	100	1.7
9.2	4.7	11.0	$7.1\cdot10^{-2}$	7	163	100	1.6
9.2	11.0	11.0	$7.1\cdot10^{-2}$	15	384	255	1.5

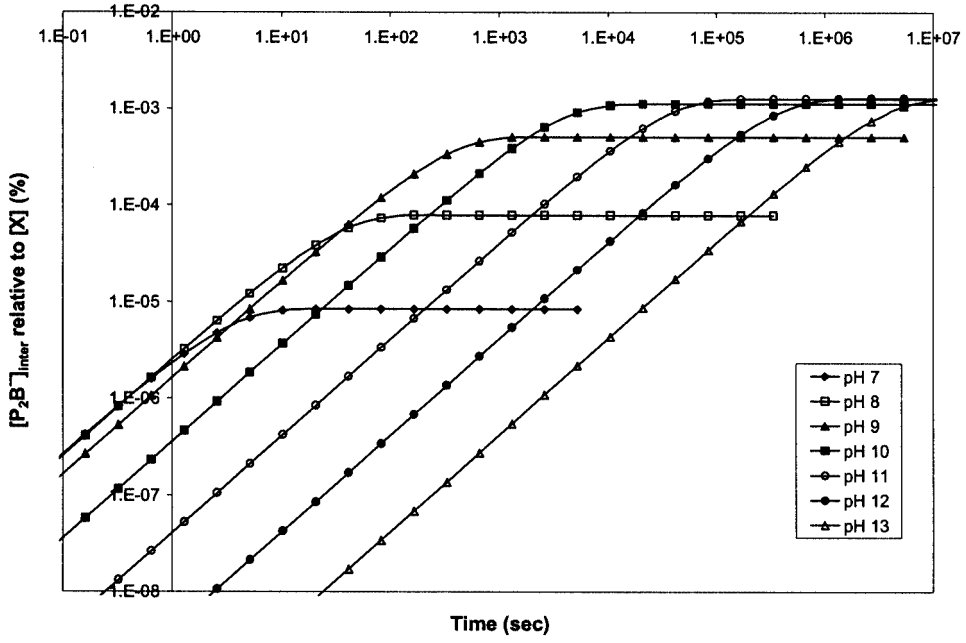

Figure 6. Results of calculated concentrations of $[X_2B^-]$ relative to the concentration of available crosslink sites X vs. time. Curves for pH values from 7 up to 13 are shown.

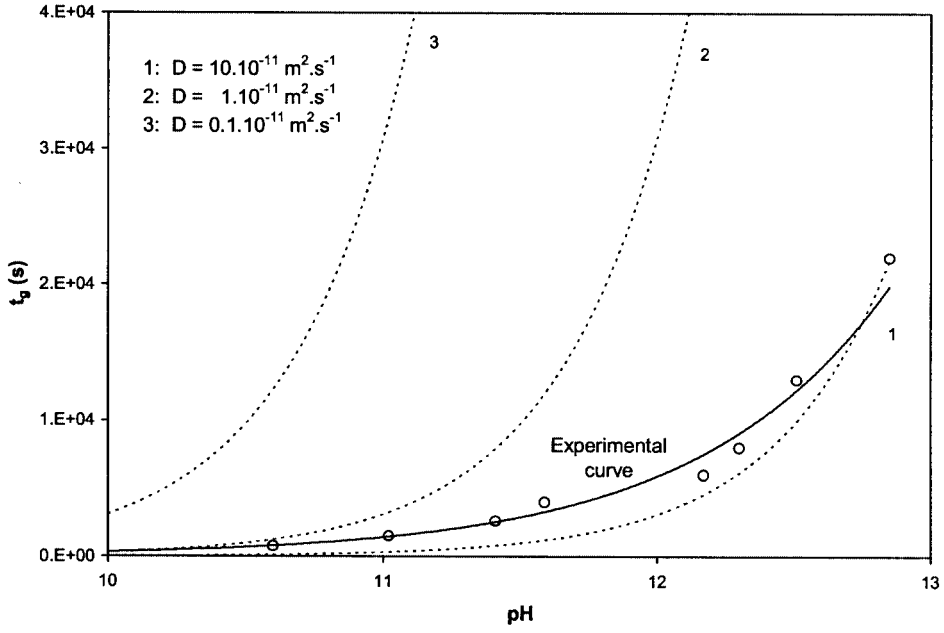

Figure 7. Results of experimental gel times as a function of pH and diffusion coefficient. Three curves (dashed) are shown based on diffusion coefficients ranging from $0.1 \cdot 10^{-11}$ $m^2 \cdot s^{-1}$ up to $10 \cdot 10^{-11}$ $m^2 \cdot s^{-1}$. The solid curve is based on experimental data.

greater. Leibler et al.[32] have made detailed calculations of these effects in reversible networks. Crosslink reactions take place between chain segments with a value for D of roughly two orders greater than the value based on sedimentation, in line with experimental data shown in Figure 7.

On the other hand, as more crosslinks form, the network becomes more rigid and consequently the mobility of the chain segments decreases.[32] As exemplified in Table 1, network formation is not much of an issue here, but it should be taken into account in experiments with more rigid gels.

The time it takes for the gel to reach maximum viscoelasticity is called the gel time, t_g, and can be calculated theoretically. The curves in Figure 6 all show the same value of the slope in a log-log plot. The value of the slope is derived by taking the ln of Equation (14a) and calculating the derivative to ln(t). Using the approximation $e^{C_2 t} \approx 1 +$

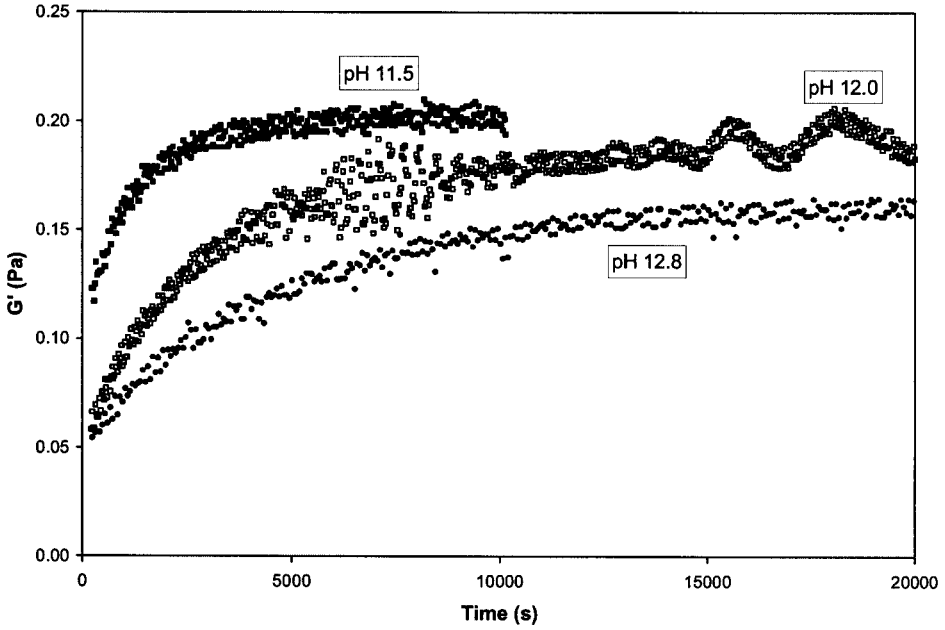

Figure 8. Results of experimental G' values as a function of time. Only a few curves measured at different pH values are shown as examples. Note that only the initial parts of the curves at pH values of 12.0 and 12.8 are shown.

$C_2 \cdot t$, it turns out that the slope is exactly 1. In Figure 6 we can draw two imaginary lines, one through the first part of the curve with a slope of 1 and one through the horizontal part with a slope of zero. The gel time is defined as the intersection of the two lines and yields:

$$t_g = \frac{1}{k_{-2} \cdot [H^+]} \tag{17}$$

These results can be translated to gel times as a function of pH and D_{guaran}. In Figure 7, three curves (dashed) are shown for different diffusion coefficients of chain segments (0.1-, 1- and $10 \cdot 10^{-11}$ $m^2 \cdot s^{-1}$). The resemblance with the experimental curve is quite reasonable, with a value of D close to $10 \cdot 10^{-11}$ $m^2 \cdot s^{-1}$, i.e., about 2 orders in magnitude greater than based on the sedimentation value but in agreement with calculations published by Leibler et al.[32]

Example experimental gel time curves are shown in Figure 8 to demonstrate the increase of gel times in tests at higher pH values. A log-log plot of the initial part of these curves shows a straight line as shown in Figure 9. The re-

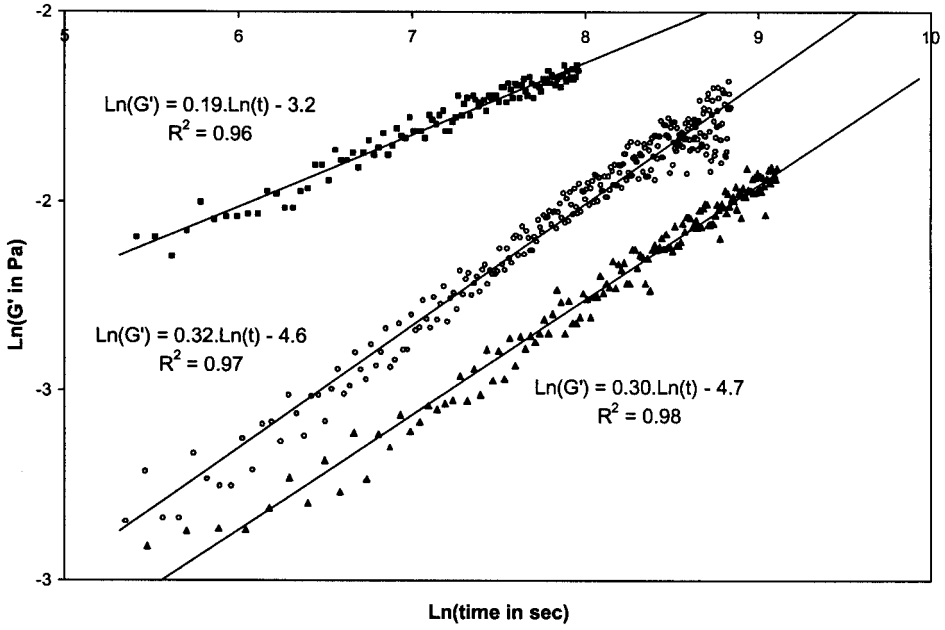

Figure 9. Calculations of the slopes of the initial parts of the curves for the examples shown in Figure 8.

sults for the gel times and the slopes of tests run at pH values >10.5, which have sufficiently long gel times, are shown in Table 3 (corrected for physical crosslinking).

Table 3. Values of the slopes of the initial part of the experimental curves and the gel times t_g

pH	Slope	Gel time (s)
10.60	0.12	750
11.02	0.19	1500
11.41	0.16	2600
11.59	0.19	4000
12.17	0.32	6000
12.30	0.30	8000
12.51	0.24	13000
12.85	0.30	22000

Compared to the theoretical value of the slope, which is exactly 1, the experimental values are < 1. The slopes of the lines increase as the pH increases but level off at a pH around 12. At low pH values, the gel time is short, and therefore the slopes could have already leveled off to some extent. This is also true in the theoretical curves. At high pH values, 12 for instance, where deprotonation of the polymer is not expected to play any role and where the network is not built up fully because the gel time is at least one hour, the value of the slope is only 0.3. This reason for this discrepancy is not clear.

Data presented in a paper by Pezron et al.[2] provide further indication of the overall correctness of the proposed mechanism. They measured G' curves as a function of frequency for gels with pH values of 8.7, 9.2, and 11. At the highest pH value tested, the plateau extends to lower frequencies and indicates longer life times of the crosslinks, in accordance with the proposed model.

Verification of Assumptions and Improvements: In the derivation of Equation (14a), the steady state assumption was applied to d([X_1B])/dt and d([X_1B^-])/dt. Using the appropriate values for k_1, k_{-1} and others the forward and reverse reaction rates were calculated for reactions 1a through 4a at pH values of 9 and 13. Compared to the B/B^- equilibrium, the relative reaction rates for the forward and reverse reactions of reaction (2a) is two orders slower, and for reaction (3a), one order slower. The forward and reverse reaction rates for reaction (4a) are five orders slower relative to the B/B^- equilibrium. Thus the assumption that the formation of X_2B^- is rate-limiting was indeed valid. Note that X_1B is replenished rapidly because X_1B^- is present in excess. A second assumption made, was constancy of [X] and [B]. As with X_1B, the concentration of B is small relative to [B^-] and readily replenished. A problem could be the amount of free available crosslink sites because a relatively large part is in the form of X_1B^-. However, relative to concentrations of available crosslink sites, model calculations show that [X_1B^-] is not even 1% at a polymer concentration of 10 g/L and a [B_t] of $1\cdot10^{-3}$M. However, in rigid gels reduction of available crosslink sites X needs to be taken into account.

Although the model has been shown to be reasonably accurate, it does have a few shortcomings: 1) in the calculation of k_{-2} application of the diffusion coefficient based on the entire polymer is unrealistic, 2) no effects due to network formation are taken into account 3) effects for the charge up of the polymer chain due to 1:1 complexes and deprotonation are not accounted for and, 4) the relation between G' and [X_2B^-] is not well defined in weakly crosslinked gels.

Verification with Results by Pezron et al.:[10] Interesting results have been compiled by Pezron et al. for borate complexes with poly(glyceryl methacrylate) by using NMR spectroscopy. This polymer was shown to have a critical polymer concentration of 20 g/L. It was observed that the ratio [X_1B^-]/[B_t] varied linearly with [P] whereas the ratio

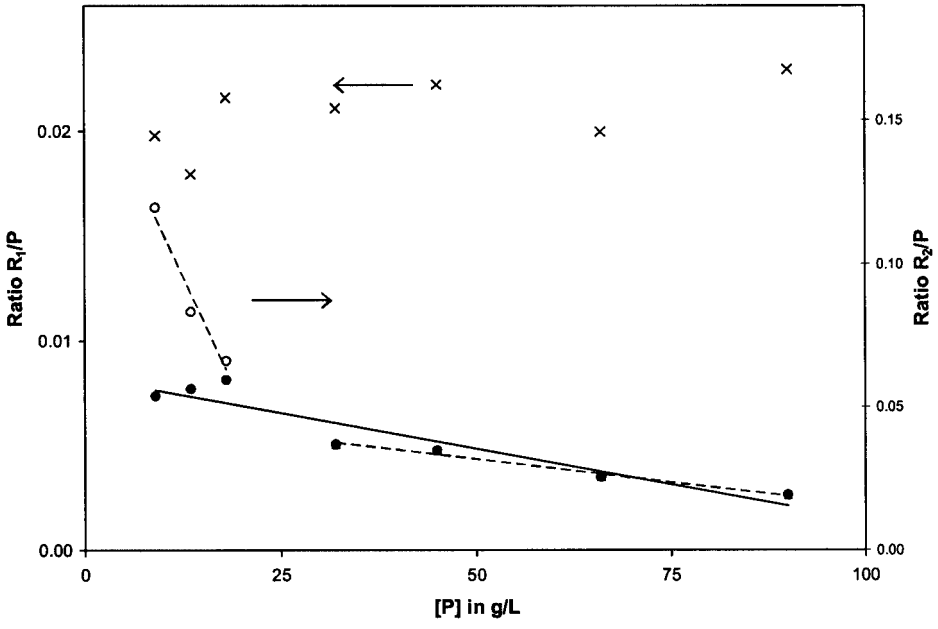

Figure 10. Results of an analysis of data published by Pezron et al.[10]; see text for details.

$[X_2B^-]/[X_1B^-]$ was independent of [P] at [P] < [P*] but dependent on [P] at [P] > [P*]. These observations are in agreement with the proposed theory, and the latter observation is especially convincing evidence for the proposed scheme of inter/intra-Mxl formation. Note that NMR does not distinguish between inter- and intra-Mxl. Thus the peak representing free boron is the sum of [B] and $[B^-]$ and the peak representing the 1:1 complex is the sum of $[X_1B^-]$ and $[X_1B]$. The first relation, $[X_1B^-]/[B_t]$, is calculated as:

$$R_1 = \frac{[X_1B^-]}{([B]+[B^-])} = \left(\frac{K_1}{K_a+[H^+]}\right)\cdot[X] \quad (18)$$

Thus R_1 divided by [P] is constant as shown in Figure 10. The second ratio R_2 is calculated as:

$$R_2 = \frac{[X_2B^-]}{[X_1B^-]+[X_1B]} = \left(\frac{K_2}{K_a^{1:1}+[H^+]}\right)\cdot[X] \quad (19)$$

and therefore R_2/[P] is constant also. However, note that the concentration of X in Equation (18) originates from the formation of 1:1 complexes and is always [X] whereas the concentration of X in Equation (19) is based on the formation of 2:1 complexes and is [X*] at [P] < [P*] and [X] at [P] > [P*], in agreement with Pezron's observations.

The dashed lines in Figure 10 represent the uncorrected data, that is, the value of [P] is used in Equation (19) for all data points. The solid line represents the corrected data, i.e., for the first three data points [P*] was used and for the remaining data points [P]. The slight decrease of the slope could be due to a reduction of the dielectric constant of the solvent at high polymer concentrations.[15]

The data shown by Pezron et al. for 1,2-propanediol are in perfect agreement with Equation (18) and (19). In this case the value of [P] can be used throughout because small molecules are able to diffuse through the entire fluid as 1:1 and as 2:1 complexes.

Verification with Results by Pizer et al.:[11–13] Attempts to clarify the mechanism have been undertaken by the group of Pizer. One observation that can be explained directly from the mechanism above is the relation between the acidity of boric acid derivatives and the value of K_1. Some data published by Pizer et al.[11] are shown graphically in Figure 11 including the results from regression analysis. A linear relationship between the pK_1 and the pK_a is observed with a slope of almost equal to 1. Note that the 95% confidence interval for the slope is quite broad and about ±0.3. Thus even though smaller slopes are suggested, its values are not statistically different from 1, the theoretical value. This latter value is readily seen if we express K_1 as $K'_1 \cdot K_a$ or $\log K_1 = \log K_a + \log K'_1$. Of course, deviations can be expected in case boron is hybridized differently.

Experimental Section

Materials: Hydroxpropyl guaran (HPG) with a molecular weight of about $2.0 \cdot 10^6$ Daltons and an MS of 0.4 was used. The HPG sample is coated with a small amount of Na-borate to improve its dispersability in water. The B-content was determined with Inductively Coupled Plasmaspectrometry (ICP) as 0.328 mg B/g polymer. As a borate source $Na_2B_8O_{13} \cdot 4H_2O$ was used in a concentration of exactly 6 g/100 g in deionized water. This solution has a density of 1.036 g/mL and contains 13.97 g B/L. For the preparation of gels, tap water was used which contains small amounts of Na^+, K^+, Mg^{2+}, Ca^{2+} and B. The content of these elements, as determined with ICP, were 49.5, 4.10, 10.2, 49.0, and 0.624 mg/L, respectively. It is known that Ca^{2+}, and probably Mg^{2+} as well, can be sequestered by 2:1 polysaccharide-borate complexes. This leads to increased values of the complex formation constant K_2. However, at these low concentrations, the effect is negligible and is therefore of no concern.[33] In the calculations, the total B content was taken into account from all three sources: tap water, polymer coating, and crosslinker solution. A 25% (w/v) solution of NaOH was used for pH adjustments. $NaHCO_3$ was added to the gels as a buffer in

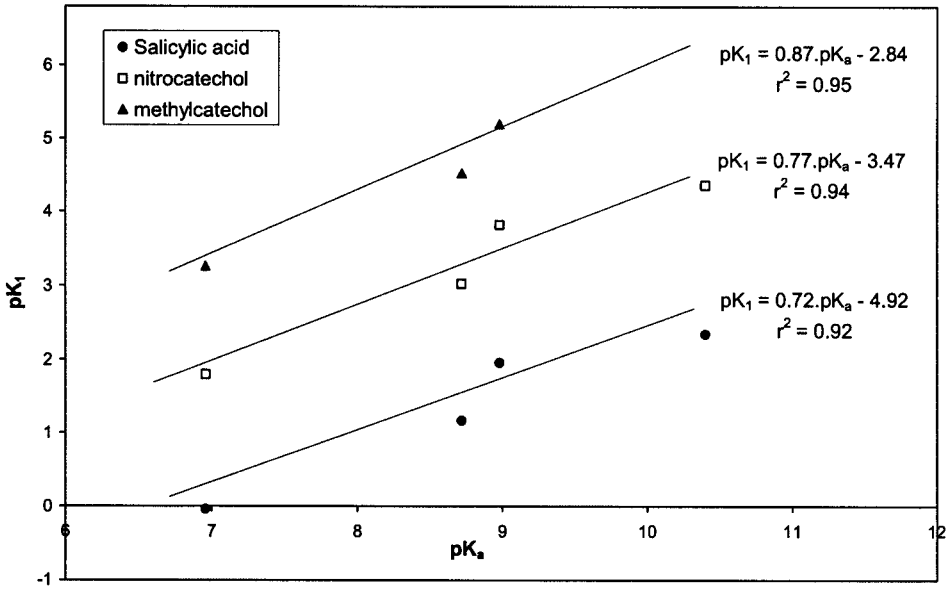

Figure 11. Results of an analysis of data published by Pizer et al.[11]; see text for details.

a concentration of exactly 3 g/kg. The reagents mentioned above were all of technical purity.

ICP Analysis: ICP was used to analyze the polymer for B and the tap water for Na^+, K^+, Mg^{2+}, Ca^{2+}, and B. The measurements were performed on a Philips PU7000 ICP. Plastic measure flaks were used to minimize the uptake of B from glassware. Exactly 10 mL of a 30% HNO_3 (p.a. quality) solution was added to the tap water samples together with 1.000 mL of a 1000 mg/L solution in Y (Merck) as an internal standard. The HPG sample was analyzed by adding 50.00 g of a base gel containing exactly 3 g/kg in DI water to a measure flask of 100 mL and adding HNO_3 and Y as above. These samples were mixed and, prior to work up, the polymer was allowed to de-polymerize in the course of about two days.

Gel Preparation: Base gels were prepared using a blade stirrer to first disperse the polymer. HPG masses from 15 to 36 g, but exactly known, were mixed in 5.000 kg tap water To initiate hydration of the polymer, the Na-borate coating was removed by adding acetic acid until a pH value of 6.5. The gel was allowed to hydrate for 15 minutes while being stirred before the sample was put in a refrigerator to further hydrate overnight. Then, the gel was homogenized and approximately 950 g of the base gel was added to a Waring blender followed by the required amount of crosslinker solution (see above), usually 500 μL. After 1 minute of stirring, 3.000 g of $NaHCO_3$ was added as a buffer, and after dissolution the pH was adjusted to the desired value with a 25% NaOH solution. In cases where gel formation was followed at high pH values (>11.5) about 75% of the required amount of NaOH was added very quickly to prevent premature gel formation. The Waring blender was then weighted off to exactly 1 kg with base gel and allowed to fully homogenize for 2 more minutes. Then the timer was started, and a sample was injected into the cup of the rheometer. Only in cases where the pH > 10.5 and the [polymer] > 3 g/L, volume and density effects due to additions of NaOH and polymer were signficant and corrected for.

The procedure above is similar for the determination of visco-elasticity due to physical crosslinks but no additional crosslinker was added and 10.0 g fructose per kg base gel was added to absolutely ascertain masking of present borate. The complex formation constant of borate with fructose (F) was determined at K'_1 = 6000 L/mol, defined as $[F_1B^-]/([B^-]\cdot[F])$, which is much higher than the constant for mannose.[6] Effective masking of borate by fructose was verified experimentally by adding 500 μL crosslinker solution to these gels: no crosslinking took place. The data were corrected for volume and density effects caused by fructose addition.

Rheology: A Reologica Stresstech rheometer was used. After the cylindrical cone plate bob was positioned, the sample was covered with a thin layer of aliphatic oil (Shellsol D90) to prevent dehydration of the gel. The gel properties G', G'' and the viscosity were followed in time by oscillating the bob at a frequency of 1 Hz and a strain of 0.3. Previous work by Pezron[2] has shown that a frequency of 1 Hz is sufficiently fast compared to the live time of the crosslinks, i.e., $(\omega.\tau)^2 >> 1$ and G' values are determined at the plateau level in all experiments. The temperature was fixed at 25.0 °C ± 0.2. The gels prepared contained relatively low concentrations of B and polymer to extend reaction times as much as possible.

Acknowledgements

We thank Drs. Gerard Glasbergen and Dr. Marco Verlaan for the useful discussions and remarks. Dr. Diederik van Batenburg and Dr. Jim Weaver are appreciated for reviewing the manuscript and the suggestions they have made. Finally, we appreciate and thank Halliburton management for permission to publish this paper.

[1] P. C. Harris, *J. Petr. Technology* **1993**, 264–269.
[2] E. Pezron, A. Ricard, L. Leibler, *J. Polym. Sci.: Polym. Phys. Ed.* **1990**, *28*, 2445–2461.
[3] R. K. Schultz, R. R. Myers, *Macromolecules* **1969**, *2*, 281–285.
[4] H. Maier, M. Anderson, K. Karl, K. Magnuson, in: *Industrial gums: polysaccharides and their derivatives*, (Eds.: R. L. Whistler, J. N. BeMiller,), Academic Press, San Diego, 3rd ed., **1993**, chapter 8.
[5] J. C. Dawson, *Soc. Petr. Eng.*, paper no. 22837, Annual Conference and exhibition of the Society of Petroleum Engineers, Dallas, Texas, October 6–9, **1991**.
[6] R. van den Berg, J. A. Peters, H. van Bekkum, *Carbohydr. Res.* **1994**, *253*, 1–12.
[7] M. van Duin, J. A. Peters, A. P. G. Kieboom, H. van Bekkum, *Tetrahedron* **1985**, *41*, 3411–3421.
[8] E. Pezron, A. Ricard, F. Lafuma, R. Audebert, *Macromolecules* **1988**, *21*, 1121–1125.
[9] E. Pezron, L. Leibler, F. Lafuma, *Macromolecules* **1989**, *22*, 2656–2662.
[10] E. Pezron, L. Leibler, A. Ricard, F. Lafuma, R. Audebert, *Macromolecules* **1989**, *22*, 1169–1174.
[11] L. Babcock, R. Pizer, *Inorg. Chem.* **1980**, *19*, 56–61.
[12] R. Pizer, L. Babcock, *Inorg. Chem.* **1977**, *16*, 1677–1681.
[13] S. Friedman, R. Pizer, *J. Am. Chem. Soc.* **1975**, *97*, 6059–6062.
[14] T. Y. Cheng, F. Rodriquez, *J. Appl. Polym. Sci.* **1981**, *26*, 3895–3908.
[15] S. W. Sinton, *Macromolecules* **1987**, *20*, 2430–2441.
[16] L. L. Khomutov, N. K. Kolnibolotchuk, E. P. Korchagina, S. A. Glikman, *J. Appl.Chem. USSR* **1967**, *40*, 1395–1399.
[17] M. van Duin, J. A. Peters, A. P. G. Kieboom, H. van Bekkum, *Tetrahedron* **1984**, *40*, 2901–2911.
[18] J. A. Peters, Technical University of Delft, private communication.
[19] F. A. Cotton, G. Wilkinson, *Advanced inorganic chemistry*, 4th ed., John Wiley & Sons, New York, **1980**, chapter 9.
[20] L. Paál, *Acta Chim. Acad. Sci. Hung.* **1977**, *95*, 31–40.
[21] T. L. Paál, *Acta Chim. Acad. Sci. Hung.* **1980**, *103*, 181–191.
[22] J. L. Frahn, *J. Chromatogr.* **1984**, *314*, 167–181.
[23] M. van Duin, J. A. Peters, A. P. G. Kieboom, H. van Bekkum, *J. Chem. Soc. Dalton Trans.* **1987**, *8*, 2051–2057.
[24] W. R. Gilkerson, *J. Chem. Phys.* **1957**, *61*, 914–917.
[25] K. Skoog, D. M. West, *Fundamentals of analytical chemistry*, 3rd ed. (Eds.: Holt, Reinhart, Winston), New York, **1976**, p. 784.
[26] J. March, *Advanced organic chemistry*, 3rd ed., John Wiley & Sons, New York, **1985**, p. 220, 221.
[27] R. Belcher, G. W. Tully, G. Svelha, *Anal. Chim. Acta* **1970**, *50*, 261–267.
[28] M. D. Lechner, E. N. Nordmeier, D. G. Steinmeier, in: *Polymer Handbook* (Eds.: J. Brandrup, E. H. Immergut, E. A. Grulke), John Wiley & Sons, New York, 4th ed., **1999**, chapter VII, p. 156.
[29] F. M. Goycoolea, E. R. Morris, M. J. Gidley, *Carbohydr. Polym.* **1995**, *27*, 69–71.
[30] F. Oosawa, *Polyelectrolytes*, Marcel Dekker, Inc., New York, **1971**, chapter 6.
[31] H. Ochiai, Y. Kurita, I. Murakami, *Makromol. Chem.* **1984**, *185*, 167–172.
[32] L. Leibler, M. Rubinstein, R. H. Colby, *Macromolecules* **1991**, *24*, 4701–4707.
[33] M. van Duin, J. A. Peters, A. P. G. Kieboom, H. van Bekkum, *J. Chem. Soc. Perkin Trans. 2* **1987**, *4*, 473–478.

Received: August 3, 2004

